Chemical Engineering Journal 259 (2015) 574–580

Contents lists available at ScienceDirect

Chemical Engineering Journal

journal homepage: www.elsevier.com/locate/cej

# Modelling and optimization of a bioremediation system utilizing silica gel encapsulated whole-cell biocatalyst

Baris R. Mutlu [a], Sujin Yeom [b], Lawrence P. Wackett [b,c], Alptekin Aksan [a,c,*]

[a] Department of Mechanical Engineering, University of Minnesota, Minneapolis, MN 55455, USA
[b] Department of Biochemistry, Molecular Biology and Biophysics, University of Minnesota, Minneapolis, MN 55455, USA
[c] BioTechnology Institute, University of Minnesota, St. Paul, MN 55108, USA

## HIGHLIGHTS

- A 3-step method is proposed for optimal design of encapsulated whole-cell biocatalysts.
- Whole-cell biocatalyst activity is characterized, including the effect of alcohol.
- Increased biocatalyst loading increased diffusivity in the silica gel.
- Increased biocatalyst loading decreased mechanical properties of the silica gel.
- Optimal biocatalyst loading and material size was determined for an encapsulated biocatalyst.

## ARTICLE INFO

*Article history:*
Received 1 April 2014
Received in revised form 25 July 2014
Accepted 31 July 2014
Available online 17 August 2014

*Keywords:*
Bioremediation
Encapsulation
Whole-cell biocatalyst
Silica gel
AtzA
Atrazine

## ABSTRACT

In this study, a 3-step design and optimization method is presented for a bioremediation system utilizing silica gel encapsulated whole-cell biocatalyst. Characterization experiments were conducted to determine the parameters of a steady state reaction/diffusion model for encapsulated AtzA biocatalyst that was subsequently verified experimentally. Dimensionless numbers governing the reaction rate, the Thiele modulus ($\Phi$) and effectiveness factor ($\eta$), were evaluated based on the design parameters of the material, $\rho$ (cell loading density) and $L_c$ (characteristic length). Mechanical properties of the gel were determined as a function of $\rho$. Optimal values for $\rho$ and $L_c$ were determined for a case study, based on biocatalytic performance, mechanical properties and cost. It was found that free biocatalyst reaction kinetics are first order with $k'_{free} = 7.38 \times 10^{-2}\ s^{-1}/(g\ cells/mL)$ and diffusivity of atrazine in the gel increases with $\rho$, from $3.51 \times 10^{-4}\ mm^2/s$ up to $6.93 \times 10^{-4}\ mm^2/s$. Modeling results showed that ~20% of activity was lost during encapsulation. Diffusion limitations became significant ($\Phi > 1$) when $L_c$ exceeded 0.1–0.3 mm. The optimal catalyst radius and cell loading density were determined to be $L_c = 0.2$ mm and $\rho = 0.11$ g cells/mL gel, for an atrazine bioremediation setup with a desired effluent <3 ppb.



## 1. Introduction

Silica gel encapsulation of biocatalysts (*i.e.* bioencapsulation) have been extensively studied in the last decade [1]. Silica gel bioencapsulation provides a robust mechanical structure and protection to otherwise fragile biocatalysts (enzymes or whole cells), which makes the technology more applicable to a wider range of engineering applications. In addition, many studies report long-term stabilization and possible enhancement to catalytic activity after encapsulation [2]. A major focus of these studies has been material and process design: Investigating biocompatible sol–gel routes [3,4], incorporating biocompatible polymers [5,6] and improving the encapsulation process to preserve and enhance biocatalytic activity. The possibility of using biocatalytic materials synthesized by silica gel bioencapsulation for water bioremediation applications have also been investigated [7–9].

In order to utilize a biocatalytic material (*i.e.* synthesized by bioencapsulation) in a water bioremediation application, specific constraints of the system need to be considered. These constraints include performance (such as the desired effluent concentration), material/operation costs (*e.g.* cost of material, biocatalyst, pumping costs) and mechanical properties (*e.g.* strength, stiffness) of the biocatalytic material. These parameters not only depend on the material, the design and the encapsulation method, but also

* Corresponding author at: Department of Mechanical Engineering, University of Minnesota, Minneapolis, MN 55455, USA. Tel.: +1 612 626 6618.
*E-mail address:* aaksan@umn.edu (A. Aksan).

http://dx.doi.org/10.1016/j.cej.2014.07.130
1385-8947/

depend significantly on the independent design parameters such as biocatalyst loading density ($\rho$) and characteristic length (*i.e.* size and geometry) of the material ($L_c$). Therefore, determining the optimal values for these design parameters are essential for successful utilization of the biocatalytic material in a large scale industrial bioremediation application.

In this study, we proposed an optimization method to determine the design parameters: $\rho$ and $L_c$, for a bioremediation system. This system is comprised of a flow through packed bed bioreactor, filled with biocatalytic material (silica gel encapsulated AtzA biocatalyst). The proposed method consists of three steps (Fig. 1). First step is the experimental characterization of the catalytic activity of the free cell biocatalyst and the permeability/mechanical properties of silica gel. For encapsulation of a free cell biocatalyst, these properties of the gel need to be investigated as a function of $\rho$. This necessity arises from the micron scale size of the free cell biocatalyst, significantly affecting the microstructure of the mesoporous silica network. Second step is the development of a steady-state reaction/diffusion model for the encapsulated cells and experimental verification of this model. Last step is the optimization of the design parameters for the bioremediation system, using constraints on performance, mechanical properties and cost. There have been previous studies where the dependence of Thiele modulus ($\Phi$) and the effectiveness factor ($\eta$) of encapsulated cells in alginate matrices have been investigated by varying $\rho$ [10] or $L_c$ [11–13]. However a method to use this information in a bioreactor setting, while satisfying biocatalytic performance, mechanical properties of the material and cost constraints to optimize $\rho$ and $L_c$ has not been established. Furthermore, silica gel encapsulation provides some unique differences such as production of ethanol during encapsulation (which affects cell membrane permeability) and strict inhibition of cell proliferation.

Atrazine (2-chloro-4-ethylamine-6-isopropylamino-*s*-triazine) is a widely used herbicide in the U.S., up to 36,000 tons annually, along with other parts of the world such as Canada, Africa and the Asia–Pacific region [14]. Its concentration is regulated by the U.S. Environmental Protection Agency (EPA) to 3 ppb in drinking water [15], and thus, bioremediation is of great practical importance. Currently, atrazine is removed from the drinking water by adsorptive filtration methods, most commonly using activated carbon that has to be disposed of or recharged by incineration with some loss of the material, added cost and $CO_2$ release. The biocatalyst used in this study is a recombinant *Escherichia coli* (*E. coli*) strain overexpressing the atrazine dechlorinating enzyme AtzA that transforms atrazine to hydroxyatrazine.

Our research group has previously shown that silica gel encapsulated AtzA biocatalyst can sustain its atrazine degradation activity over 4 months [16]. We have also shown that AtzA biocatalyst can be encapsulated in different geometries including slabs, spherical beads or electrospun PVA/silica nanofibers [17]. When utilized in a spherical bead form in a flow through packed bed reactor bioremediation system, continuous degradation activity at low ppb concentrations of atrazine was achieved [18]. In this study, we propose an optimal design for the biocatalytic material to satisfy specific performance constraints, such as reaching the desired 3 ppb limit in the effluent with a sustained influent AtzA concentration of 10 ppb, while ensuring high mechanical integrity of the system at a low cost.

## 2. Materials and methods

### 2.1. Materials

Reagent grade tetraethoxysilane (TEOS: $Si(OC_2H_5)_4$) was purchased from Sigma–Aldrich (Sigma–Aldrich Corp., St. Louis, MO, USA). NexSil 125-40 silica nanoparticle (SNP) sol was purchased from Nyacol (Nyacol Nano Technologies Inc., Ashland, MA, USA). Analytical grade atrazine was provided by Syngenta (Syngenta Crop. Protection, NC, USA). All chemicals were used without further purification. Ultrapure water (UPW) was used in all the experiments, which was prepared by filtering deionized water through a Milli-Q water purification system (Millipore, Billerica, MA, USA) to a final electrical resistance of >18.2 MΩ/cm.

### 2.2. Bacterial strains and growth conditions

The growth conditions were identical to those described previously [16], except for some minor modifications as described below. *E. coli* strain DH5α (pMD4) [19] was grown at 37 °C in superbroth medium with vigorous aeration. The medium was supplemented with 30 μg/ml chloramphenicol. Intermediate cultures were grown by inoculation with 1% (v/v) starter culture and diluted 100-fold in production flasks containing the same medium. Cells were harvested by centrifugation at 6000 g for 20 min at 4 °C.

### 2.3. Silica gel synthesis and encapsulation of cells

A previously reported silica gel matrix (NS125-7:1-TEOS) and encapsulation method was used in this study [18], where the cells are well-entrapped in the silica matrix and are not able to proliferate. Briefly, TEOS was hydrolyzed by stirring (2 h) at a 1:5.3:0.0013 M ratio of TEOS:water:HCl. The pH of the Nexsil 125-40 SNP sol was adjusted to neutrality by adding 1 M hydrochloric acid. After pH adjustment, bacteria were suspended in phosphate buffered saline (1 g cells/mL PBS) and added to the SNP sol. Hydrolyzed TEOS was added to the bacteria and SNP solution by pipetting a few times to obtain a homogeneous sample. The final

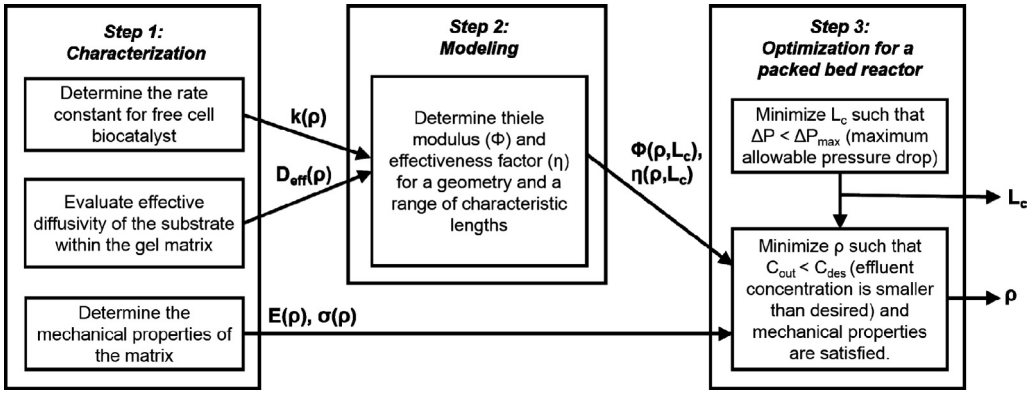


**Fig. 1.** Design algorithm for determining optimal cell loading density ($\rho$) and characteristic length ($L_c$) for silica gel encapsulated biocatalyst.

product was either placed in silicone molds (for mechanical testing) or in 20 mL scintillation vials (for activity testing) for gelation.

### 2.4. Characterization of free cell AtzA catalyst reaction kinetics

It was previously reported that free AtzA enzyme obeys Michaelis–Menten (MM) kinetics and its $K_m$ and $V_{max}$ values were determined [19]. To apply these values for kinetic modeling of an intact cell containing AtzA, one would need to have good estimates of parameters such as: enzyme concentration in the cell, cell membrane permeability and diffusivity of atrazine/hydroxyatrazine in the cell. Instead, we used a more convenient approach by developing a free cell model that does not require explicit knowledge of these parameters. We also investigated the effect of ethanol (a by-product of silica gel synthesis), on cell membrane permeability and free cell kinetics.

A 0.003 g aliquot of cells suspended in PBS was added to 5 mL ($\rho = 6 \times 10^{-4}$ g cells/mL) of an atrazine solution (concentration of atrazine ranged from 30 to 150 μM) prepared with 0.1 M potassium phosphate buffer (at pH 7.0) in a 20 mL scintillation vial. Scintillation vials were placed on a rotary shaker and incubated for 20 min. After incubation, samples were collected and immediately immersed in a 90 °C water bath to stop the catalytic activity by denaturing the enzyme. After inactivation of the enzyme, samples were filtered through a 0.2-μm pore size PTFE syringe filter to remove the cells. The concentrations of atrazine and its metabolite, hydroxyatrazine, were measured by using high performance liquid chromatography (HPLC) as described by de Souza et al. [19]. HPLC results were converted to concentrations using calibration curves for atrazine (0–150 μM, 30 μM increments, $R^2 = 0.9986$) and hydroxyatrazine (0–80 μM, 20 μM increments, $R^2 = 0.9999$).

In order to evaluate the effects of ethanol concentration, a similar procedure was followed with minor changes. Three mL buffer solutions were prepared with ethanol concentrations ranging from 1% to 50% (v/v). Sonicated cell suspension was obtained by immersing a sonicator tip into the free cell suspension and operating it at 30% power, 5s on–off intervals for 90 s. After sonication, sonicated cell suspension was centrifuged to separate the supernatant with cytoplasmic proteins from the cell membrane fragments. Then, 0.03 g of non-sonicated free cells and 50 μL of supernatant solution (0.005 g cell extract) from sonicated cells were added to the buffer solutions (separately) with ethanol and were incubated for an hour. After incubation, 2 mL of 150 μM atrazine solution was added ($\rho_{free} = 6 \times 10^{-3}$ g cells/mL and $\rho_{sonicated} = 1 \times 10^{-4}$ g cell extract/mL) to a final concentration of 90 μM and vials were incubated for 20 min. The remainder of the assay procedure was identical.

### 2.5. Determination of atrazine transport in silica gel matrix

The silica gel matrix was synthesized as a thin cylindrical disk (diameter = 7.5 mm, thickness = 3 mm). One side of the disk was exposed to a reservoir filled with 150 μM atrazine solution in 0.1 M potassium phosphate buffer, and the other side was exposed to water. After 24 h of exposure, samples were collected to determine the amount of atrazine that permeated through the membrane from the atrazine reservoir to the water reservoir. In order to investigate the possible effect of cell loading on the matrix permeability, silica gel disks with wild-type cells (that do not express AtzA) were synthesized as a control. Cell loading density ($\rho$) values of 0.11, 0.20, 0.33, 0.43 and 0.5 g cells/mL gel were tested. Rest of the experimental procedure was identical to the cell-free disk case.

### 2.6. Evaluation of the mechanical properties

Cylindrical test pieces of silica gel matrix with a thickness of 12 mm and a diameter of 12 mm were synthesized using a silicone mold. After 24 h of aging in the mold, the samples were air dried for another 24 h for easy removal from the molds. It was observed that the sample diameter decreased from 12 mm to 11.4 ± 0.1 mm during this process. After removal from the mold, samples were rehydrated by immersion in PBS before the mechanical testing on an MTS QTest 10 machine (MTS Systems, Eden Prairie, MN, USA). Compressive strength ($\sigma$) and elastic modulus for compression ($E$) of the material were evaluated by compression tests conducted on the hydrated samples at 1%/min strain rate. Cell-free samples and samples with cells ($\rho = 0.059$, 0.11, 0.20, 0.33 g cells/mL gel) were tested in quadruplicate. Samples were determined to be too weak for practical purposes beyond $\rho = 0.33$ g cells/mL for mechanical testing and therefore not tested.

### 2.7. Experimental verification of reaction/diffusion model

Silica gel matrix with encapsulated cells was synthesized as a cylindrical slab (gel thickness = 7 ± 0.1 mm) at the bottom of a 20 mL scintillation vial. The experiments were conducted immediately after gelation and no changes in dimensions were observed due to shrinkage or swelling of the gel. Five different cell loading density ($\rho$) values were tested (0.03, 0.059, 0.11, 0.20, 0.33 g cells/mL gel) in triplicate. Three mL atrazine solutions (in 0.1 M potassium phosphate buffer) at 150 μM concentration were added to the scintillation vials. Vials were placed on a rotary shaker and incubated for 20 min. After incubation, solution was removed, replaced with fresh atrazine solution and incubated for another 20 min. This "re-spiking" procedure was repeated 5 times, until further atrazine adsorption to the silica gel matrix has stopped (as verified by mass balance) so that steady state degradation was achieved. In preliminary studies (data not shown), it was observed that atrazine adsorption to silica gel matrix reduced the observed activity rates. This is because the atrazine transport within the matrix is hindered by adsorption of atrazine to silica gel. Therefore, minimizing adsorption by re-spiking yielded an accurate estimation of the steady-state activity rates. Note that this re-spiking procedure also removes any cells, which may have been leaked from the gels during gelation. The experimental measurements of activity were then compared to the predictions of the reaction/diffusion model developed.

The aim of the developed model is to successfully estimate the steady-state biocatalytic activity of encapsulated cells, based on cell loading density ($\rho$), characteristic length ($L_c$), and geometry of the material. Two dimensionless numbers can be used to estimate the steady-state performance of encapsulated catalysts: Thiele modulus ($\Phi$) and the effectiveness factor ($\eta$) [20]. $\Phi$ is the ratio of characteristic reaction rate to characteristic diffusion rate. Small values of $\Phi$ ($\Phi \ll 1$) correspond to reaction-limited catalysis while large values of $\Phi$ ($\Phi \gg 1$) correspond to diffusion-limited catalysis. $\eta$ is the ratio of observed reaction rate ($r_{obs}$) to maximum reaction rate ($r_{max}$), which would only be achieved in the absence of internal diffusion limitations. Mathematically, these two dimensionless numbers are expressed as follows:

$$\Phi \equiv L_c \sqrt{\frac{k'_{free} * \rho}{D_{eff}}} \tag{1.a}$$

$$\eta \equiv \frac{r_{obs}}{r_{max}} \tag{1.b}$$

Note that $k'_{free}$ (or $k'_{enc}$ which can also be used in Eq. (1.a)) and $D_{eff}$ need to be determined in characterization studies. $\eta$ can also be analytically derived as a function of $\Phi$, for different encapsulation geometries. For slab and spherical geometries, $\eta$ can be written in terms of $\Phi$ as [20]:

$$\eta = \frac{\tanh(\Phi)}{\Phi} \quad \text{(for slab)} \tag{2.a}$$

$$\eta = \frac{3}{\Phi}\left[\frac{1}{\tanh(\Phi)} - \frac{1}{\Phi}\right] \text{ (for sphere)} \quad (2.b)$$

Using Eqs. (2.a) and (2.b), $\eta$ can be determined and inserted in Eq. (1.b) to get an estimation for the observed degradation rate. For verification of this model, we compared this expected degradation rate to the experimentally observed degradation rates. For modeling results, we have used two different rate constants ($k'_{free}$ and $k'_{enc}$), to demonstrate the effect of ethanol concentration on free cell activity.

### 2.8. Optimization of $\rho$ and $L_c$

For a bioremediation system, maximizing $\eta$ (or minimizing $\Phi$) is not sufficient for optimization of $\rho$ and $L_c$ because other constraints such as performance, material/operating cost and mechanical properties of the material need to be satisfied. In order to demonstrate this, a case study is considered where atrazine contaminated water is treated using a bioreactor packed with spherical biocatalysts in a flow-through setup. Table 1 shows the parameters and performance criteria used in the case study. For simplicity, external mass transfer resistances within the reactor are assumed negligible such that $C_{surface}(L) = C_{bulk}(L)$, where $C_{surface}$ is the atrazine concentration at the bead surface and $C_{bulk}$ is the concentration of the bulk flow, at a distance $L$ from the inlet of the reactor.

## 3. Results and discussion

### 3.1. Characterization

#### 3.1.1. Free cell AtzA catalyst reaction kinetics and effect of ethanol concentration on activity

Fig. 2a shows that up to the solubility limit of atrazine in water (in the 30–150 μM range) the enzymatic reaction transforming atrazine into hydroxyatrazine is of first order. Therefore, the free cell model takes the following form:

$$r = k_{free}(\rho)C_{Atrazine} = k'_{free}\rho C_{Atrazine} \quad (3)$$

where $C_{Atrazine}$ is the atrazine concentration in [μM], $k_{free}$ ($\rho$) is the degradation rate constant for free cells at a given cell loading density [$s^{-1}$], $k'_{free}$ is the degradation rate constant for free cells per cell loading density [$s^{-1}$/(g cells/mL)] and $r$ is the reaction rate in [μmole/L-s].

Using the experimental parameters ($\rho = 6 \times 10^{-4}$) and a least-squares-regression analysis, we determined that $k_{free} = 4.43 \times 10^{-5}\ s^{-1}$ and incorporating $\rho$, we get $k'_{free} = 7.38 \times 10^{-2}\ s^{-1}$/(g cells/mL). For verification of these results, we obtained an activity value per cell mass using experimental parameters (5 mL solution, 0.003 g cells) and an initial atrazine concentration of 150 μM. This leads to an activity rate of 0.66 μmole/(g cells min), which is in accord with our previously reported free cell activity of 0.61 ± 0.04 μmole/(g cells min) measured at 150 μM atrazine concentration [16].

Fig. 2b shows that both $k'_{free}$ (free cells) and $k'_{sonicated}$ (sonicated cells) change significantly with changing ethanol concentration ($C_{EtOH}$). It can be immediately observed that $k'_{sonicated}$ is an order of magnitude higher than $k'_{free}$ when $C_{EtOH} = 0\%$, which shows the effect of transport limitations caused by the cellular membrane and intracellular transport. It can also be observed that the activity loss with increasing $C_{EtOH}$ is more significant with sonicated cells compared to free cells, since there is no protection offered to the free enzyme by the intracellular environment. A peak can be observed around $C_{EtOH} = 30\%$ for free cells, which can be attributed to increased permeability of the cell membrane due to ethanol damage.

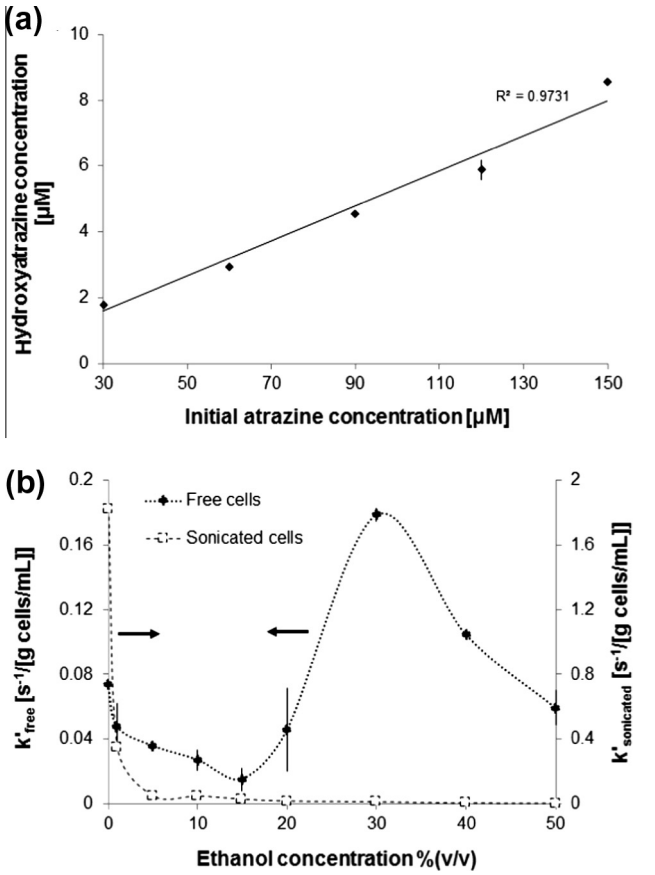


**Fig. 2.** (a) Free cell AtzA biocatalyst activity (at $\rho = 6 \times 10^{-4}$ g cells/mL solution, 20 min incubation time). (b) Effect of ethanol concentration on biocatalyst activity rate constant ($k'_{free}$).

Assuming full hydrolysis and condensation, we can estimate the ethanol concentration in the synthesized gel to be approximately 5% (v/v). Then, using Fig. 2b, a new rate constant for encapsulated cells as $k'_{free@5\%\ EtOH} = k'_{enc} = 3.58 \times 10^{-2}\ s^{-1}$/(g cells/mL) can be obtained to be used in the reaction/diffusion model.

#### 3.1.2. Atrazine diffusivity in silica gel matrix

Fig. 3 shows that atrazine has a diffusivity of $D_{eff} = 3.51 \times 10^{-4}$ $mm^2/s$ within the silica gel matrix (an order of magnitude lower than that of water in water [21]: $2.3 \times 10^{-3}$ $mm^2/s$) without encapsulated cells. In contrast, Trypan blue dye (MW: 873 Da) has a diffusivity of $D_{eff} = 2.25 \times 10^{-4}$ $mm^2/s$ in the same silica gel matrix [18], therefore it was expected that atrazine (MW: 218 Da) had a

**Table 1**
Parameters used in the packed bed reactor case study.

| | | | |
|---|---|---|---|
| Influent atrazine concentration ($C_{in}$) | 50 ppb | Reactor volume ($V$) | 10 L (400 $cm^2$ × 25 cm) |
| Desired output concentration ($C_{out}$) | <3 ppb | Packing density ($\varepsilon$) | 0.6 |
| Flow-rate ($Q$) | 1 L/min | Fluid properties ($\mu$, $\rho_f$) | Water properties at 20 °C |
| Cost of cells | 0.1 $/g cells | | |

higher diffusivity due to its smaller molecular size. It was observed that increasing cell loading density ($\rho$) increased the permeability of the gel to atrazine. To incorporate this into the model, the following correlation, derived from the data presented in Fig. 3 was used to estimate the diffusivity of the matrix for a given $\rho$ as follows:

$$D_{\text{eff}} = (7.23 \times 10^{-4})\rho + (3.46 \times 10^{-4})\ \text{mm}^2/\text{s} \quad (4)$$

Based on (4), it can be seen that diffusivity of atrazine in the gel increased with increased cell loading density ($\rho$), from $3.51 \times 10^{-4}$ mm$^2$/s up to $6.93 \times 10^{-4}$ mm$^2$/s. We suspect that this phenomenon could be due to increased transport of atrazine through: (a) cell-silica interface within the matrix, (b) the cells themselves. Due to this effect, $\rho$ not only affects the biocatalytic activity rate constant, but also the transport of atrazine in the matrix.

### 3.1.3. Compressive strength ($\sigma$) and elastic modulus ($E$)

Fig. 4 shows that cell free silica gels have $\sigma \approx 1.75$ MPa, $E \approx 160$ MPa. It can also be seen that both $\sigma$ and $E$ of the material deteriorate with increased $\rho$, down to $\sigma \approx 0.28$ MPa, $E \approx 23$ MPa at the maximum tested $\rho$ (0.33 g cells/mL gel). Both $\sigma$ and $E$ showed an exponential decreasing trend with the following least-square fit correlations:

$$\sigma = 1736.5e^{-5.5\rho}[\text{kPa}] \quad (5.a)$$

$$E = 182.19e^{-5.966\rho}[\text{MPa}] \quad (5.b)$$

### 3.2. Model verification

Fig. 5 shows that the experimentally observed activity was lower than the expected activity of the model when ethanol-free rate constant ($k'_{\text{free}}$) is used. This result suggests that 19.7 ± 10.2% of cell degradation activity was lost during encapsulation. When 5% ethanol medium rate constant ($k'_{\text{enc}}$) is used, the observed activity was higher than the expected activity (116.7 ± 14.7%). This result suggests that the alcohol content of the gel is overestimated or some alcohol evaporated during gelation. Even though expected activity with $k'_{\text{enc}}$ was slightly lower than the experimentally observed activity, it was still used for optimization purposes, to ensure that the performance constraints of the system is met.

### 3.3. Optimization of design parameters $\rho$ and $L_c$

Fig. 6 shows the range of attainable operating conditions for a spherical biocatalyst in terms of $\Phi$ and $\eta$, for $0.01 < \rho < 1$ g cells/mL gel and $0.1 < L_c < 10$ mm. Fig. 6a shows that as $L_c$ increases, $\Phi$

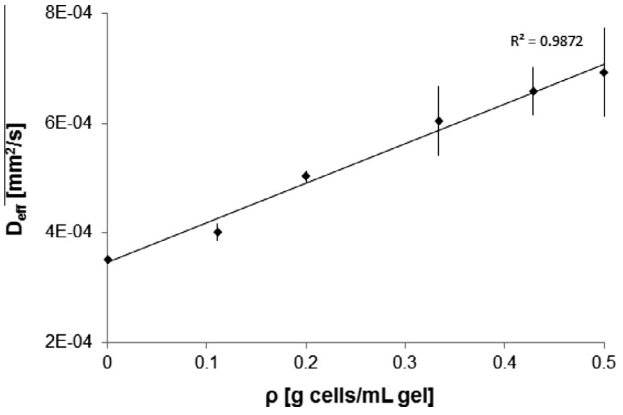


**Fig. 3.** Change in gel diffusivity to atrazine ($D_{\text{eff}}$) as a function of cell loading density ($\rho$).

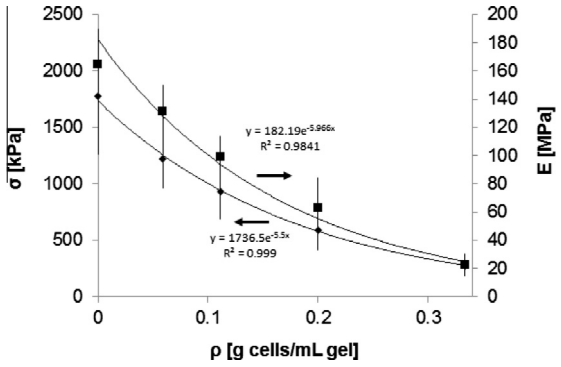


**Fig. 4.** Mechanical properties of the gel (maximum yield strength ($\sigma$) and elastic modulus ($E$)) as a function of cell loading density ($\rho$).

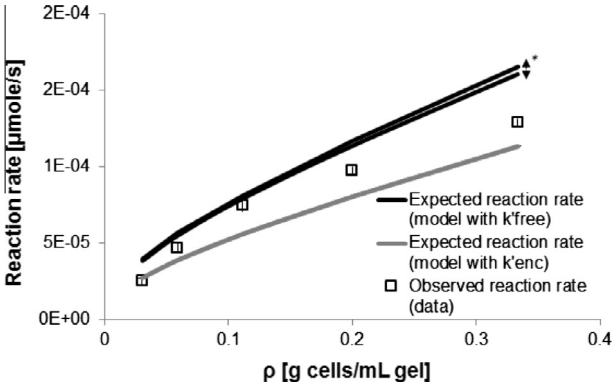


**Fig. 5.** Steady-state model verification (* indicates the uncertainty in the expected reaction rate due to experimental variation in slab thickness).

also increases, indicating that diffusion limitations become more severe as material gets larger, as expected. As $\rho$ increases, $\Phi$ also increases, and the effect is more significant at large values of $L_c$. Fig. 6c shows that the increasing trend in $\Phi$ reflects a decrease in $\eta$, which can also be seen from Eq. (2.b). Two-dimensional projections of Fig. 6a and c are shown in Fig. 6b and d for ease of visualization. The inset in Fig. 6b shows that diffusion limitations become significant ($\Phi > 1$) when $L_c$ of the material (sphere radius) exceeds 0.1–0.3 mm, depending on $\rho$. Fig. 6d shows that for a typical bead radius of 1 mm, AtzA biocatalyst reaction is severely diffusion limited and only 35% (at $\rho = 1$ g cells/mL gel) to 90% (at $\rho = 0.01$ g cells/mL gel) of the material can be utilized.

### 3.3.1. Optimization of $L_c$

It is apparent from Fig. 6 that $L_c$ should be minimized to decrease the diffusion limitations, regardless the material geometry or reactor type. However, in a packed bed setup, minimizing $L_c$ is not desirable due to increased pressure drop, which would increase initial cost (high pressure pump, high pressure reactor design) and operating costs (pumping cost) of the system. Fig. 7a shows the pressure drop vs. catalyst size for a range of volumetric flow-rates, based on Ergun equation [22]:

$$\frac{\Delta P}{L} = \frac{150\mu(1-\varepsilon)^2 u_0}{\varepsilon^3 (2L_c)^2} + \frac{1.75(1-\varepsilon)\rho_f u_0^2}{\varepsilon^3 (2L_c)} \quad (6)$$

where $\mu$ is the fluid viscosity, $\rho_f$ is fluid density, $u_0$ is superficial velocity of the fluid and $L$ is the length of the reactor. Due to this pressure drop, instead of minimizing $L_c$, it is more practical to set a lower bound on $\eta$ and pick the corresponding catalyst size. $\eta = 0.9$ is a reasonable selection that ensures 90% utilization of the

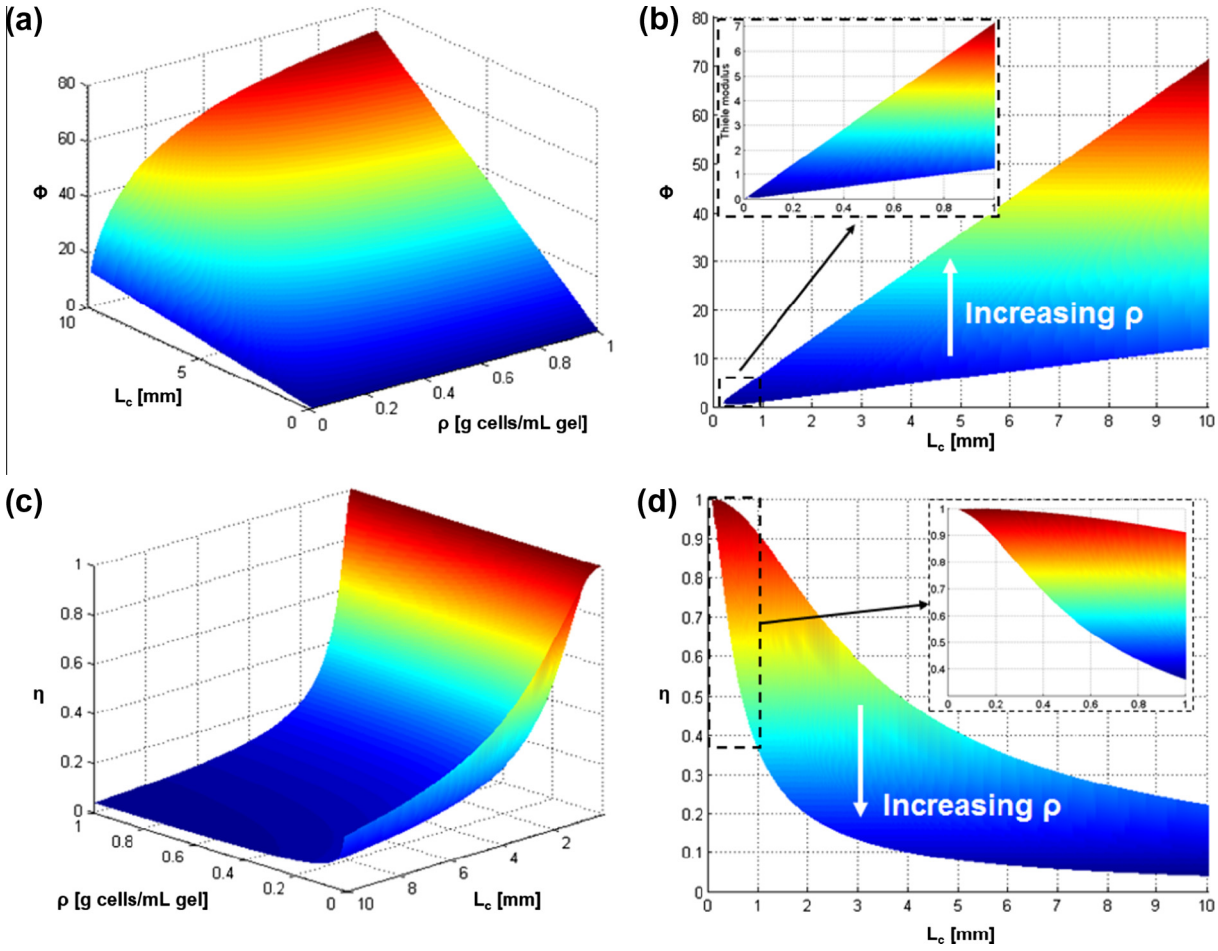


**Fig. 6.** Variation of dimensionless numbers: $\Phi$ (a,b) and $\eta$ (c,d), based on design parameters: $\rho$ and $L_c$.

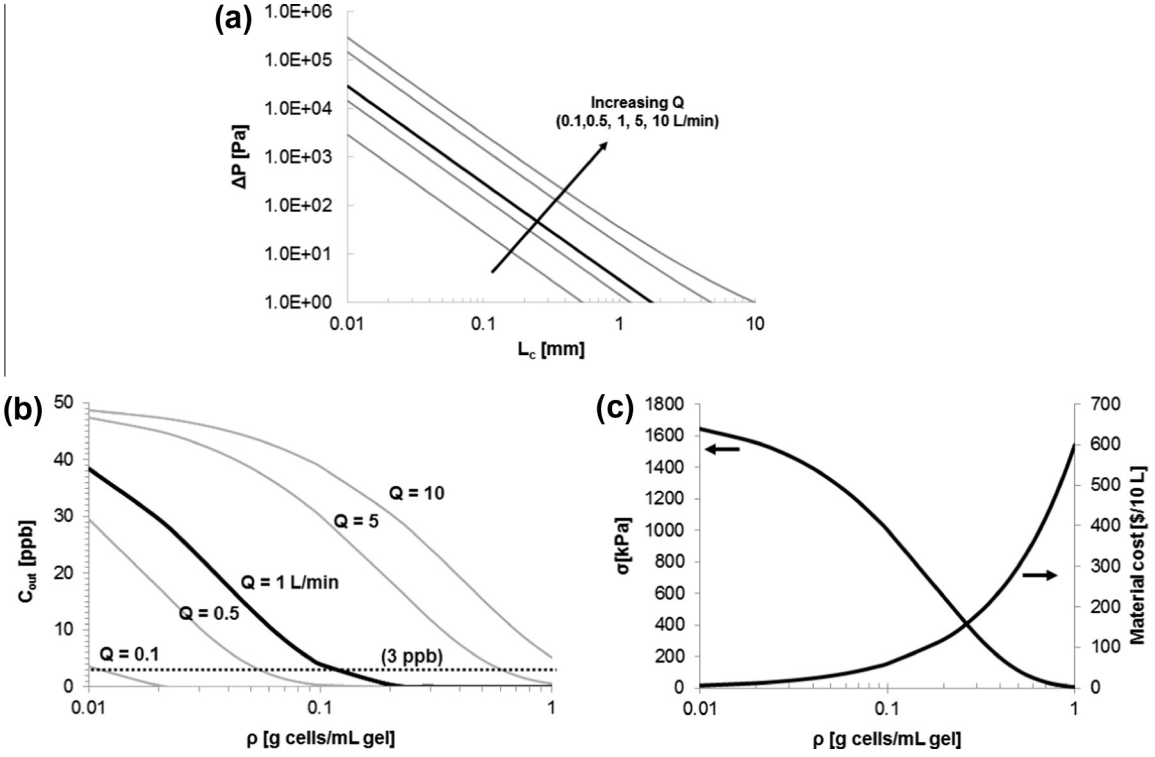


**Fig. 7.** (a) Pressure drop ($\Delta P$) across the packed bed reactor based on $L_c$. (b) Effluent concentration ($C_{out}$) of the packed bed reactor based on $\rho$ and flow-rate ($Q$). (c) Maximum yield strength ($\sigma$) and total material cost based on $\rho$.

**Table 2**
Minimum, maximum and optimal values of $\rho$ and $L_c$.

| | Minimum value | Maximum value | Optimal value |
|---|---|---|---|
| $L_c$ | Imposed by $\Delta P$ across the reactor (Fig. 7a) | Imposed by $\eta$ (Fig. 6d) | Minimum value satisfying $\Delta P < \Delta P_{max}$ (maximum allowable pressure drop) |
| $\rho$ | Imposed by performance constraint of the system (Fig. 7b) | Imposed by material properties and cost of the material (Fig. 7c) | Minimum value satisfying $C_{out} < C_{des}$ (desired effluent concentration) |

material. The inset of Fig. 6d shows that if a minimum of $\eta = 0.9$ is selected, the optimal value for catalyst radius is $L_c = 0.2$ mm, regardless of $\rho$.

### 3.3.2. Optimization of $\rho$

Minimizing $\rho$ is desirable to increase effectiveness factor, obtain enhanced mechanical properties and decrease material cost; whereas it should still be large enough such that performance constraints of the system are satisfied. For a packed bed reactor operating at steady-state, the output concentration is given by [23]:

$$C_{out} = C_{in} e^{\frac{-\varepsilon V \eta(\rho) k_{enc}(\rho)}{Q}} \quad (7)$$

Note that both $\eta$ and $k_{enc}$ changes with $\rho$. Fig. 7b shows the change in output concentration of the packed bed reactor as a function of $\rho$, for the selected optimal catalyst size $L_c = 0.2$ mm and a range of volumetric flow-rate values ($Q = 0.1$–$10$ L/min). It can be seen that to obtain the desired output concentration lower than 3 ppb, $\rho$ must be greater than 0.11 g cells/mL gel (for $Q = 1$ L/min). Fig. 7c shows that to minimize the cost and maximize mechanical strength of the material, minimum $\rho$ value that satisfies the performance constraint should be selected. Then, for this case study, $\rho = 0.11$ g cells/mL gel is the optimal cell loading density, which yields $\sigma = 578$ kPa and a material cost of $120 to fill up a 10 L reactor.

In this case study, optimal design parameters ($L_c = 0.2$ mm and $\rho = 0.11$ g cells/mL gel) were selected to minimize material cost and pressure drop, maximize material strength while satisfying a performance constraint for a given reactor size and flow-rate ($Q$). Selection criteria of these parameters are summarized in Table 2. It can be seen that if any of these constraints are relaxed and other constraints are imposed on the system, Fig. 7a–c can still be used to determine values for $L_c$ and $\rho$, which satisfy these requirements. Otherwise, they can also be used to determine that all the constraints cannot be satisfied at once and one or more of the requirements need to be relaxed.

## 4. Conclusion

In this study, we proposed a 3-step [(1) characterization, (2) modeling, (3) optimization] design approach for determining cell loading density ($\rho$) and characteristic length ($L_c$) of silica gel encapsulated AtzA biocatalyst used in a packed bed bioremediation system. The approach was to maximize mechanical properties and minimize material/operation cost, while satisfying performance requirements of the bioremediation system. This 3-step approach is demonstrated for a case study, whose parameters are described in Table 1. The proposed method to choose minimum, maximum and optimal values of these design parameters are summarized in Table 2. Note that Table 2 is not specific to silica gel encapsulated AtzA biocatalyst, and can be used for other biocatalytic materials. However, this requires a corresponding characterization and modeling step, as described in this study.

## Acknowledgements

We acknowledge the support of an NSF-IIP/PFI Grant (#1237754), an NSF-CAREER award (#0644784), a research grant from Syngenta Crop Protection and MnDrive fellowship to BRM from the BioTechnology Institute in University of Minnesota.

## References

[1] D. Avnir, T. Coradin, O. Lev, J. Livage, Recent bio-applications of sol–gel materials, J. Mater. Chem. 16 (11) (2006) 1013–1030.
[2] A.C. Pierre, The sol–gel encapsulation of enzymes, Biocatal. Biotransform. 22 (3) (2004) 145–170.
[3] A. Leonard, J.C. Rooke, C.F. Meunier, H. Sarmento, J.-P. Descy, B.-L. Su, *Cyanobacteria* immobilised in porous silica gels: exploring biocompatible synthesis routes for the development of photobioreactors, Energy Environ. Sci. 3 (3) (2010) 370–377.
[4] M.L. Ferrer, L. Yuste, F. Rojo, F. del Monte, Biocompatible sol–gel route for encapsulation of living bacteria in organically modified silica matrixes, Chem. Mater. 15 (19) (2003) 3614–3618.
[5] N. Nassif, C. Roux, T. Coradin, M.N. Rager, O.M.M. Bouvet, J. Livage, A sol–gel matrix to preserve the viability of encapsulated bacteria, J. Mater. Chem. 13 (2) (2003) 203–208.
[6] N. Nassif, A. Coiffier, T. Coradin, C. Roux, J. Livage, O. Bouvet, Viability of bacteria in hybrid aqueous silica gels, J. Sol–Gel. Sci. Technol. 26 (1–3) (2003) 1141–1144.
[7] M. Perullini, M. Jobbagy, N. Mouso, F. Forchiassin, S.A. Bilmes, Silica–alginate–fungi biocomposites for remediation of polluted water, J. Mater. Chem. 20 (31) (2010) 6479–6483.
[8] T. Branyik, G. Kuncova, J. Paca, K. Demnerova, Encapsulation of microbial cells into silica gel, J. Sol–Gel. Sci. Technol. 13 (1–3) (1998) 283–287.
[9] A. Pannier, M. Mkandawire, U. Soltmann, W. Pompe, H. Bottcher, Biological activity and mechanical stability of sol–gel-based biofilters using the freeze-gelation technique for immobilization of Rhodococcus ruber, Appl. Microbiol. Biotechnol. 93 (4) (2012) 1755–1767.
[10] P. Kaul, A. Banerjee, U.C. Banerjee, Stereoselective nitrile hydrolysis by immobilized whole-cell biocatalyst, Biomacromolecules 7 (5) (2006) 1536–1541.
[11] Z. Aksu, G. Bulbul, Determination of the effective diffusion coefficient of phenol in Ca-alginate-immobilized P-putida beads, Enzyme Microb. Technol. 25 (3–5) (1999) 344–348.
[12] T.P. Chung, H.Y. Tseng, R.S. Juang, Mass transfer effect and intermediate detection for phenol degradation in immobilized *Pseudomonas* putida systems, Process Biochem. 38 (10) (2003) 1497–1507.
[13] A. Laca, C. Quiros, L.A. Garcia, M. Diaz, Modelling and description of internal profiles in immobilized cells systems, Biochem. Eng. J. 1 (3) (1998) 225–232.
[14] N.D. Jablonowski, A. Schaeffer, P. Burauel, Still present after all these years: persistence plus potential toxicity raise questions about the use of atrazine, Environ. Sci. Pollut. Res. 18 (2) (2011) 328–331.
[15] Interpreting the Atrazine Drinking Water Monitoring Data <http://www.epa.gov/oppsrrd1/reregistration/atrazine/atrazine_update.htm>.
[16] E. Reategui, E. Reynolds, L. Kasinkas, A. Aggarwal, M.J. Sadowsky, A. Aksan, L.P. Wackett, Silica gel-encapsulated AtzA biocatalyst for atrazine biodegradation, Appl. Microbiol. Biotechnol. 96 (1) (2012) 231–240.
[17] H.-W. Tong, B.R. Mutlu, L.P. Wackett, A. Aksan, Silica/PVA biocatalytic nanofibers, Mater. Lett. 111 (2013) 234–237.
[18] B.R. Mutlu, S. Yeom, H.-W. Tong, L.P. Wackett, A. Aksan, Silicon alkoxide cross-linked silica nanoparticle gels for encapsulation of bacterial biocatalysts, J. Mater. Chem. A 1 (36) (2013) 11051–11060.
[19] M.L. De Souza, M.J. Sadowsky, L.P. Wackett, Atrazine chlorohydrolase from *Pseudomonas* sp. strain ADP: Gene sequence, enzyme purification, and protein characterization, J. Bacteriol. 178 (16) (1996) 4894–4900.
[20] M.E. Davis, R.J. Davis, Fundamentals of Chemical Reaction Engineering, Dover Publications, 2012.
[21] J.R. Jones, D.L.G. Rowlands, C.B. Monk, Diffusion coefficient of water in water and in some alkaline earth chloride solutions at 25 °C, Trans. Faraday Soc. 61 (1965) 1384–1388.
[22] P. Harriott, Chemical Reactor Design, Taylor & Francis, 2002.
[23] R.L. Fournier, Basic Transport Phenomena in Biomedical Engineering, Taylor and Francis, 2011.